Simulation of MEMS Energy Harvesting Generators Based on Bennet's Doubler

Antonio Carlos M. de Queiroz
COPPE/EP – Electrical Engineering Program
Federal University of Rio de Janeiro
Rio de Janeiro, Brazil
acmq@ufrj.br

Luiz Carlos Macedo de Oliveira Filho
EP-Department of Electronic and Computer Engineering
Federal University of Rio de Janeiro
Rio de Janeiro, Brazil
eng.luizmof@poli.ufrj.br

***Abstract*—This paper presents considerations about the design and operation of electrostatic generators based on Bennet's doubler, when realized with microelectromechanics techniques. Electrical models taken from mechanical analogs are used to simulate the devices in operation, with the effects of the mechanical operations and interactions with electrical forces taken into account in the models. From the simulated results, guidelines for the design of the actual systems can be obtained.**

Keywords—energy harvesting; microelectromechanics; electrostatics; low-power circuits

I. INTRODUCTION

The design of microgenerators based on variable capacitances for energy harvesting using microelectromechanic systems (MEMS) is quickly advancing, with devices that are similar to big capacitive accelerometers being used for this purpose [1], [2], [3]. With small devices the generated power is very small, but can be enough to power devices that operate in intermitent way, as sensors that communicate by radio. These devices are usually based on a single variable capacitor, and require a high-voltage bias, using electrets as bias generators for variable capacitor generators, or at least a battery for initial precharging, that is recharged by the generator. A different approach, initially described in [4], [5], is to use a true "influence machine", an unstable electrostatic generator, to create exponentially growing voltages as a sequence of back-and-forth or rotational movements is repeated. The device proposed for this was a modification of the simplest of these machines, the "doubler of electricity", described by Abraham Bennet in 1787 [6]. Its schematic diagram is shown in Fig. 1, comprising two variable capacitors C_a and C_b, a storage capacitor C_1, and three diodes. When the two variable capacitances are varied cyclically in complementary way, the device generates an exponentially growing voltage in C_1. C_b can be fixed, at the expense of larger capacitance variation in C_a required. In the several "macroscopic" implementations so far tested [5], [7], the devices were observed to start without any explicit initial charge, just from natural charge imbalances, generating in a few cycles an output voltage only limited by sparking between the plates, at several kV.

In this work, the construction or the doubler in MEMS technology is studied, with some possible structures considered. They are investigated through simulation models that treat the mechanical devices using electrical analogs in a locally developed simulator, with the objective of finding the required parameters for the MEMS devices, starting from the desired electrical behavior.

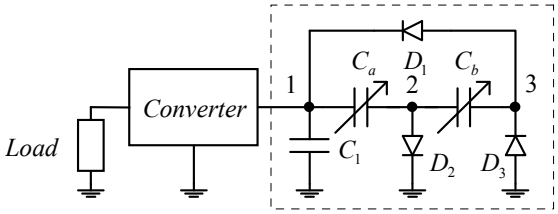

Fig. 1. Electronic doubler of electricity connected to a load through a DC/DC converter.

II. OUT-OF-PLANE OPERATION

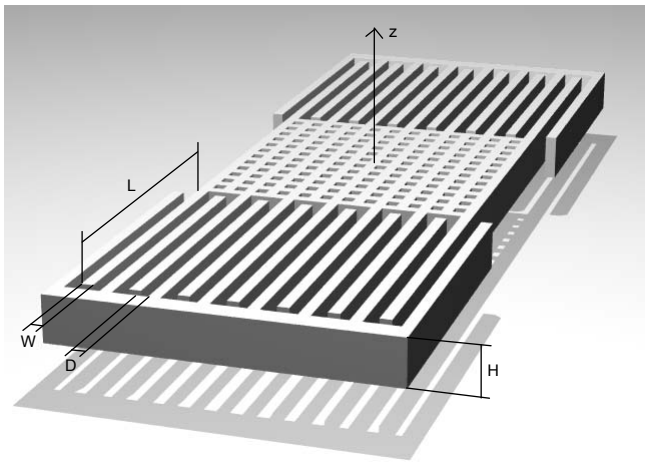

Fig. 2. MEMS structure for out-of-plane operation with overlap variation.

Figure 2 shows a possible basic layout for a MEMS device, where a moveable central block with N fingers of length L, width W, and height H at each side moves up and down, suspended by adequate springs, with the combs of fingers inserted between similar combs at each side. The separation between the fingers is always a fixed distance D. This layout keeps the capacitor plates at constant separation, with only their overlap varying. Some free space must exist above and below the moveable section, and the suspension must restrict the movement

978-1-4799-8332-2/15/$31.00

to the vertical direction. This single variable capacitor can be used as C_a, in a doubler with fixed C_b. The moveable part can be node 1, with most stray capacitances absorbed in C_1. The capacitance between the moveable part and the fixed combs, supposing that the moveable part is offset vertically by a distance z_0–z, with fringe fields ignored and $|z_0-z|<H$, is:

$$C_a = 2\frac{\varepsilon_0 L_t H}{D}\left(1-\frac{|z_0-z|}{H}\right) \quad (1)$$

where for operation in air $\varepsilon_0 = 8.85\times10^{-12}$ F/m and L_t is the total length of the gap at one side:

$$L_t = 2N(L+W+D)+W \quad (2)$$

The doubler requires significant capacitance, to overcome losses and stray capacitances and to generate useful power. 100 pF seems to be a reasonable maximum capacitance to use. For operation at high voltage, taking advantage of the high electric fields possible at small distance without the formation of sparks [8], but allowing some safety margin, a separation D = 20 µm seems reasonable. With H = 400 µm, W = 20 µm, and L = 2000 µm, from (1) and (2), L_t = 28.25 cm and N = 69 fingers at each side are required. The total length of the device is then of $(2N+1)(W+D)–D$ = 5540 µm. Assuming a square device, the width of the central block is 1540 µm. With a polysilicon density of 2330 kg/m^3, the total mass of the moveable block, including fingers, is of 13.1 mg. The springs would add some mass, but the holes in the block would take something similar, so the mass of the moveable part will be assumed as this.

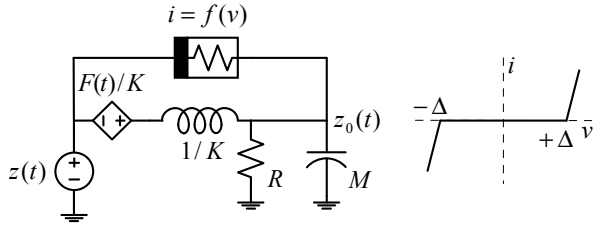

Fig. 3. Analog model for the mechanical system.

Figure 3 shows an analog electric model for the MEMS device, using an integrated version of the analog where force corresponds to current and velocity corresponds to voltage. In this case, the integral of force corresponds to current and position corresponds to voltage. A voltage source $z(t)$ models the vibration waveform, or the vertical position of the fixed combs and of the anchors of the springs supporting the moveable block. The suspension springs with spring constant K are modeled by the inductor with inductance $1/K$ and the mass M of the moveable block by the capacitor with capacitance M. A resistor R adds damping through a force proportional to the velocity of the mass. The controlled voltage source models the effect of a force directly applied to the mass, which is used to model the electrical force. This force has to be integrated in this model, but appears not integrated as shown with a Thévenin equivalent with the inductor or spring. A nonlinear resistor, with the curve $i = f(v)$ as shown, adds limits to the relative movement, clamping with low resistance the maximum difference between $z(t)$ and $z_0(t)$. The limiter does not affect the normal operation of the model in the following simulations.

The model, while the limiter is inactive, corresponds to a second-order low-pass resonant system, with resonance frequency and quality factors given by the usual expressions:

$$f_0 = \frac{1}{2\pi}\sqrt{\frac{K}{M}};\quad Q = 2\pi f_0 RM \quad (3)$$

It is assumed that with chosen f_0 and M suitable springs and damping systems can be designed so the desired Q is achieved. With f_0 = 100 Hz and Q = 4, for example, K = 5.17 N/m and R = 486 (m/s)/N. The variable capacitance has maximum value at the rest position, and decreases linearly as the moveable block moves up or down, reaching a negligible value, ideally zero, when $|z_0-z| = H$. The value of the capacitance $C_a(t)$ can be generated as a voltage by the model in Fig. 4 (the simulator used has a voltage-controlled capacitance model implemented), taking as input the positions z and z_0 from the model in Fig. 3.

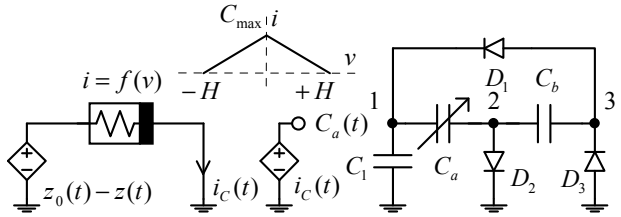

Fig. 4. Capacitance generator and doubler.

The voltage over C_a creates an attraction force opposing the displacement. This force can be calculated as the derivative of the stored energy relative to $z_0 - z$:

$$F = \frac{dE}{d(z_0-z)} = \frac{1}{2}v_{Ca}^2\frac{dC_a}{d(z_0-z)} = \pm v_{Ca}^2\frac{\varepsilon_0 L_t}{D} \quad (4)$$

The model in Fig. 5 uses voltage multipliers and a nonlinear resistor to make a sign function to calculate the force as a voltage and applies it to the capacitor representing the mass through the controlled voltage source n Fig. 3.

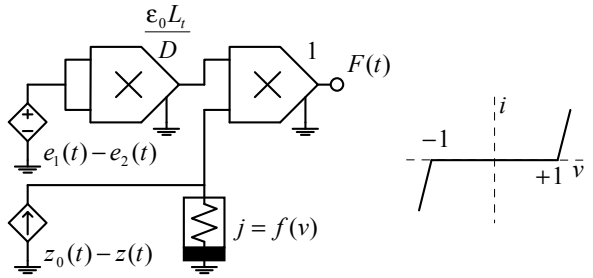

Fig. 5. Electric force generator.

The simulation of the complete system, with ideal diodes in the doubler, produces the results plotted in Figs. 6 and 7. The vibration source $z(t)$ is a sinusoid with 100 µm of amplitude. With Q = 4 the mass starts oscillating and briefly shocks against the limiters, placed at ±350 µm, while the voltage over C_1 is increases from initial 2 V by the doubler with C_a varying at a maximum of 8:1 ratio. An interesting observation is that after 100 ms the electrical force becomes strong enough to limit the movement. The capacitance variation then drops below the minimum required for unstable operation with only C_a variable, ideally 2:1, and the output voltage ceases to grow. The

ringing of the mechanical system produces an overshoot, and leakage resistors of 10 GΩ added in parallel with the diodes cause the voltages to drop until the doubler is again unstable. It reaches a steady state at its limit of stability, just replenishing the leakage, with 2:1 capacitance variation, keeping about 31 V over C_1. This phenomenon impedes the operation of the doubler with higher voltages.

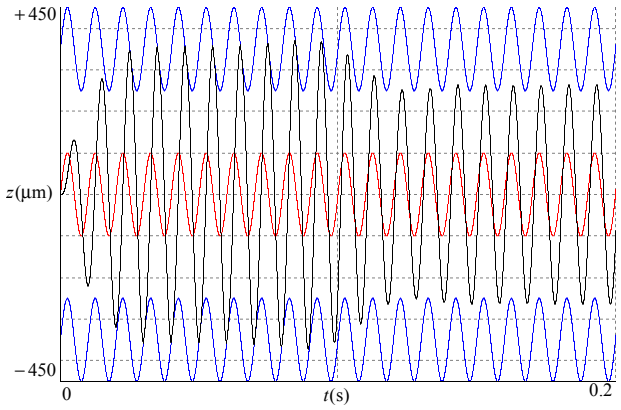

Fig. 6. Input and output displacements, showing shocks of the moveable block with the limiters above and below.

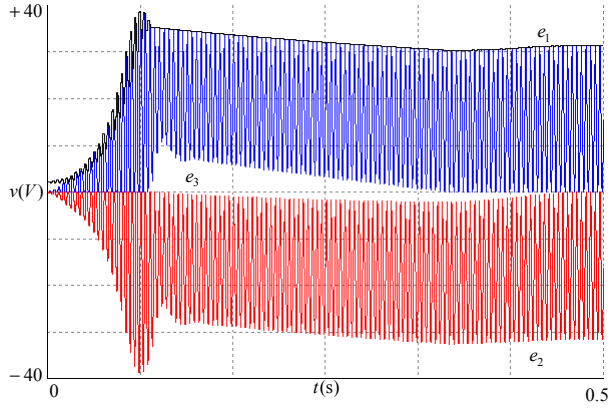

Fig. 7. Voltages at the nodes of the doubler, showing stabilization at 31 V.

The steady-state situation can be predicted, by observing that, in Fig. 3, the difference $z_0(t)$–$z(t)$ is approximately sinusoidal with amplitude $H/2$ to cause a 2:1 capacitance variation in C_a, and has a phase φ relative to $z(t)$. The electric force $F(t)$ can be also approximated as sinusoidal with amplitude F and the same phase (although it is clearly not sinusoidal). Considering the analog model network excited by $z(t)$ (a cosinusoid with amplitude z and angular frequency $\omega = 2\pi f$) and $F(t)$, using phasor representation:

$$\frac{H}{2}\cos\varphi + j\frac{H}{2}\sin\varphi = \frac{\omega_0^{\,2} z - \dfrac{F\cos\varphi + jF\sin\varphi}{M}}{-\omega^2 + j\dfrac{\omega_0}{Q}\omega + \omega_0^{\,2}} - z \quad (5)$$

This equation can be solved for F and φ by equating the real and imaginary parts. The solution when the excitation is at the angular resonance frequency, $\omega = \omega_0$, is:

$$\varphi = -\tan^{-1}\left(\frac{H}{\sqrt{4z^2(Q^2+1)-H^2}}\right) - \tan^{-1}\frac{1}{Q}$$
$$F = \frac{M\omega_0^{\,2}\sqrt{4z^2(Q^2+1)-H^2}}{2Q} \quad (6)$$

Observing (see Fig. 7) that the maximum voltage over C_a is ideally $2e_1$ when C_a varies in a 2:1 ratio, the peak value of the electric force, assumed as identical to the peak of its sinusoidal fundamental component, is:

$$F = 4e_1^{\,2}\frac{\varepsilon_0 L_t}{D} \quad (7)$$

Applying the parameters used in the simulation, (6) gives φ = –0.75 rad, or –43°, and $F = 4.66\times10^{-4}$ N. The maximum voltage that the doubler can generate is then (8). For the obtained force, the predicted e_1 is 30.6 V, very close to the simulated value. A design parameter that can be adjusted to control the maximum voltage at the doubler's output is the mass M, with the maximum output voltage depending on the square root of the mass, if the resonance frequency and the quality factor remain the same. The same happens with the distance D, but it affects the capacitance and the energy that the doubler can generate.

$$e_{1\max} = \sqrt{\frac{M\omega_0^{\,2} D\sqrt{4z^2(Q^2+1)-H^2}}{8\varepsilon_0 L_t Q}} \quad (8)$$

Similar analyses are possible for other modes of operation, as in-plane overlap changing and in-plane separation change, with corresponding changes in the geometry and equations.

III. In-Plane Operation with Complementary Capacitors

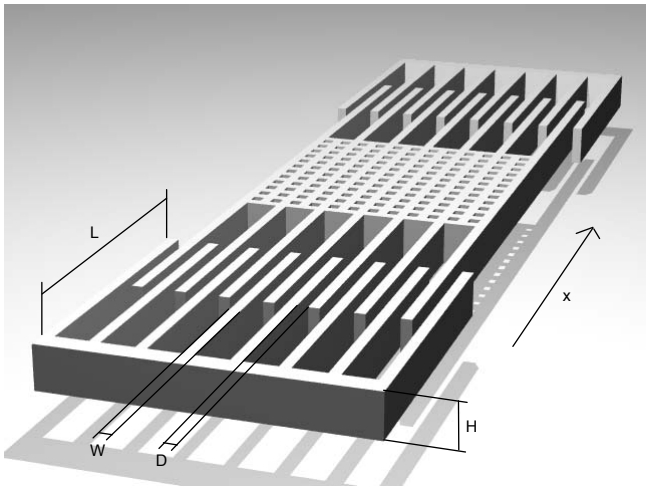

Fig. 8. MEMS structure with two complementary capacitors with in-plane overlap variation.

The doubler ideally requires less capacitance variation (1.618:1) when two capacitors varying in a complementary way are used. This can be obtained with a MEMS structure as the one shown in Fig. 8, where the overlap with the two sets of stationary fingers vary while the central block moves in the x

direction, suspended by suitable springs. The central block is then node 2 in Fig. 1, with the fixed combs being nodes 1 and 3. The model for the mechanical part is the same of Fig. 3, but with excitation $x(t)$ and block movement $x_0(t)$. Assuming that at rest the finger overlap is $L/2$ and the movements are limited to $|x_0–x| = L/2–D$, ignoring fringe fields and effects at the course limits, the capacitances vary following the relations, implemented by the model in Fig. 9:

$$C_a = \frac{\varepsilon_0 NH}{D}\left(L - 2(x_0 - x)\right);\ C_b = \frac{\varepsilon_0 NH}{D}\left(L + 2(x_0 - x)\right) \quad (9)$$

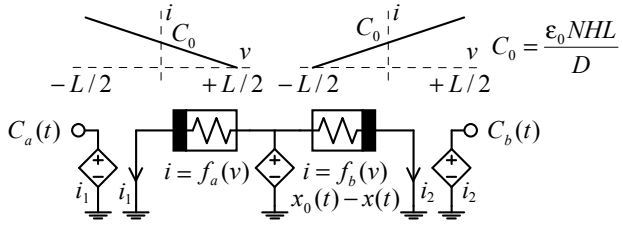

Fig. 9. Capacitance generator for two complementary capacitances.

The forces in both capacitors are then (10), with the corresponding generating model shown in Fig. 10.

$$F_a = \frac{1}{2} v_{Ca}^{\ 2}\left(-2\frac{\varepsilon_0 NH}{D}\right);\ F_b = \frac{1}{2} v_{Cb}^{\ 2}\left(2\frac{\varepsilon_0 NH}{D}\right) \quad (10)$$

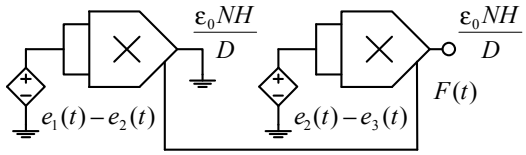

Fig. 10. Electric force generator for two complementary capacitances.

Assuming the same parameters from the previous case, the simulation of the complete system reveals that there is also a maximum output voltage limited by the electric forces, but it is easily much higher than in the first case. The electric force is always in the same direction because v_{Ca} is always larger than v_{Cb}, pulling the moveable block in the direction that increases C_a, which at steady state varies around a larger rest capacitance than C_b. The stabilization of the doubler then requires a different capacitance variation from the ideal 1.618:1 for both capacitors. The same analysis of the mechanical system applies, with some additional complexity. Equation (5) is also valid, but with $H/2$ replaced by an unknown Δx, z replaced by x, and F being the variation of the electrical force around its average value, that is approximately F too. The central block is pulled by the average electrical force by a distance approximately equal to F/K, causing symmetrical shifts in the average values of the capacitances. The capacitances can be expressed as function of Δx, and the condition of limit of stability in the doubler [5] generates another equation, that combined with the modified (6) allows the calculation of the electrical force, and from it and considerations of how the capacitances change, of the maximum output voltage. The complete analysis is too long to be shown here, and requires the numerical solving of two equations to find F and Δx. For the parameters in the example, using vibration amplitude $x = 250$ µm, the analysis results in $F = 1.29\times10^{-3}$ N and Δx of exactly 250 µm. The calculated maximum output voltage is 325 V, while the simulation gives 329 V for 100 GΩ leakage resistances. The capacitance variations result as 1.5:1 for C_a and 2:1 for C_b, exactly too. Figure 11 shows a simulation of the system. The maximum capacitances are of ~50 pF, because the two halves are used in different capacitors. $C_1 = 50$ pF was used to keep the startup fast.

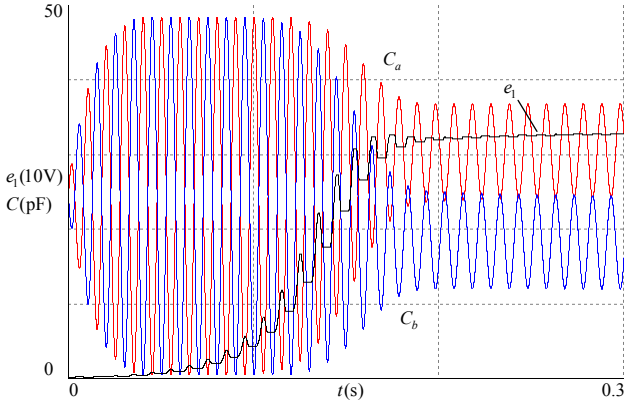

Fig. 11. Capacitances and output voltage, showing the different variations.

IV. Conclusions

Two variations of a MEMS design for a "doubler of electricity" were studied. The analyses showed that there is a limit in the maximum voltage that the devices can generate due to electrical forces. This limit can be predicted with relatively simple approximations, and must be taken into account in the design of the actual devices, because it can be easily larger than the voltage required for normal operation of the device as energy harvester.

References

[1] R. Guilllemet, P. Basset, D. Galayko, F. Cottone, F. Marty, and T. Bourouina, "Wideband MEMS electrostatic vibration energy harvesters based on gap-closing interdigited combs with a trapezoidal cross section," 2013 IEEE 26th International Conference on Micro Electro Mechanical Systems (MEMS), pp. 817-820, January 2013.

[2] A. Crovetto, F. Wang, O. Hansen, "Modeling and Optimization of an Electrostatic Energy Harvesting Device," Journal of Microelectromechanical Systems, vol. 23, no. 5, pp. 1141-1155, October 2014.

[3] V. Janicek and M. Husak, "3D electrostatic microgenerator," 2012 13th International Conference on Thermal, Mechanical and Multi-Physics Simulation and Experiments in Microelectronics and Microsystems, pp. 1-8, April 2012.

[4] A. C. M. de Queiroz, "Electrostatic vibrational energy harvesting using a variation of Bennet's doubler," 53rd Midwest Symposium on Circuits and Systems, Seattle, USA, pp. 404-407, August 2010.

[5] A. C. M. de Queiroz e M. Domingues, "The doubler of electricity used as a battery charger," IEEE Trans. on Circuits and Systems II, Vol. 58, No. 12, pp. 787-801, December 2011.

[6] A. C. M. de Queiroz, "Doublers of electricity," Physics Education, 42, pp. 156-162, March 2007.

[7] A. C. M. de Queiroz and M. S. de Souza, "Batteryless electrostatic energy harvester and control system," 2014 IEEE International Symposium on Circuits and Systems, Melbourne, Australia, pp. 1977-1980, June 2014.

[8] J.-M. Torres and R. S. Dhariwal, "Electric field breakdown at micrometre separations," Nanotechnology, vol. 10, no. 1, pp. 102–107, March 1999.